Journal of Neurochemistry, 2006, **98**, 951–961 doi:10.1111/j.1471-4159.2006.03919.x

Distribution of PINK1 and LRRK2 in rat and mouse brain

Jean-Marc Taymans, Chris Van den Haute and Veerle Baekelandt

Laboratory for Neurobiology and Gene Therapy, Division of Molecular Medicine Katholieke Universiteit Leuven, Leuven, Belgium

Abstract

Mutations in two kinases, PTEN induced kinase 1 (PINK1) and leucine-rich repeat kinase 2 (LRRK2), have been shown to segregate with familial forms of Parkinson's disease. Although these two genes are expected to be involved in molecular mechanisms relevant to Parkinson's disease, their precise anatomical localization in mammalian brain is unknown. We have mapped the expression of PINK1 and LRRK2 mRNA in the rat and mouse brain via *in situ* hybridization histochemistry using riboprobes. We found that both genes are broadly expressed throughout the brain with similar neuroanatomical distribution in mouse compared to rat. PINK1 mRNA abundance was rather uniform throughout the different brain regions with expression in cortex, striatum, thalamus, brainstem and cerebellum. LRRK2, on the other hand, showed strong regional differences in expression levels with highest levels seen in the striatum, cortex and hippocampus. Weak LRRK2 expression was seen in the hypothalamus, olfactory bulb and substantia nigra. We confirmed these distributions for both genes using quantitative RT-PCR and for LRRK2 by western immunoblot. As their broad expression patterns contrast with localized neuropathology in Parkinson's disease, the pathogenicity of clinical mutant forms of PINK1 and LRRK2 may be mediated by nigrostriatal-specific mechanisms.

Keywords: *in situ* hybridization histochemistry, leucine-rich repeat kinase 2, Parkinson's disease, PTEN induced kinase 1, quantitative RT-PCR, western blot.

J. Neurochem. (2006) **98**, 951–961.

Introduction

Parkinson's disease (PD) is the second most common neurodegenerative disease. At present, PD is incurable and its etiology is unclear. The past decade has seen much progress in the search for the molecular causes underlying Parkinson's disease, most notably by the identification of disease causing mutations in at least 5 genes. Mutations in Parkin, DJ-1 and PTEN-induced putative kinase 1 (PINK1) cause autosomal-recessive forms of PD, while mutations in α-synuclein and recently described mutations in leucine-rich repeat kinase 2 (LRRK2) cause autosomal-dominant forms of PD (Gasser 2005).

PINK1 was first discovered as a serine/threonine-type protein kinase capable of *in vitro* autophosphorylation, with differential expression in cancer cell lines with higher metastatic potential (Unoki and Nakamura 2001; Nakajima *et al*. 2003). In 2004, PINK1 was identified as the gene responsible for the PARK6 locus when 2 homozygous mutations in the kinase domain of PINK1 were identified in three PARK6 families (Valente *et al*. 2004). Since then, a number of other clinical mutations or truncations in PINK1

Received March 3, 2006; revised manuscript received March 24, 2006; accepted March 30, 2006.

Address all correspondence and reprint requests to Veerle Baekelandt, Katholieke Universiteit Leuven, Laboratory for Neurobiology and Gene Therapy, Kapucijnenvoer 33, B-3000 Leuven, Belgium.
E-mail: veerle.baekelandt@med.kuleuven.be

Abbreviations used: AcbC, accumbens nucleus, core; AcbSh, accumbens nucleus, shell; ACo, anterior cortical amygdaloid nucleus; AM, anteromedial thalamic nucleus; AV, anteroventral thalamic nucleus; BLA, basolateral amygdaloid nucleus; BLAST, basic local alignment search tool; CA1, CA1 hippocampal field; CA3, CA3 hippocampal field; COR, C-terminal of Ras of complex proteins; CPu, caudate-putamen; Cx, cortex; DG, dentate gyrus; Dienc, diencephalon; DLG, dorsolateral geniculate nucleus; Hip, hippocampus; Hyp, hypothalamus; IMLF, interstitial nucleus medial longitudinal fasciculus; KLH, keyhole limpet haemocyanin; La, lateral amygdaloid nucleus; Lat, lateral cerebellar nucleus; LGP, lateral globus pallidus; LRRK2, leucine-rich repeat kinase 2; LS, lateral septum; MAPK(KK), mitogen activated kinase (kinase kinase); Mes, mesencephalon; MS, medial septum; ob, olfactory bulb; PD, Parkinson's disease; PINK1, PTEN induced kinase 1; qRT-PCR, quantitative RT-PCR; RT-PCR, reverse transcription polymerase chain reaction; Sept, septum; sm, stria medullaris, thalamus; SNC, substantia nigra pars compacta; SNR, substantia nigra pars reticulate; Str, striatum; VTA, ventral tegmental area.

have been found (Hatano *et al*. 2004; Healy *et al*. 2004; Rogaeva *et al*. 2004; Rohe *et al*. 2004).

In 2004, mutations in LRRK2 were shown to be responsible for PARK8-linked PD (Paisan-Ruiz *et al*. 2004; Zimprich *et al*. 2004). As of today, at least 15 putatively pathogenic amino acid substitutions have been identified in LRRK2, 6 of which have been confirmed to segregate with Parkinson's disease (Mata *et al*. 2005). LRRK2 is a large multi-domain protein which has recently been confirmed to possess kinase activity (Gloeckner *et al*. 2005; West *et al*. 2005).

Because PINK1 and LRRK2 have only recently been linked to PD, studies of these two kinases in the brain are limited. Preliminary mRNA regional expression patterns using tissue extracts showed that PINK1 is expressed in human brain as well as in peripheral tissues such as heart, skeletal muscle or testis (Unoki and Nakamura 2001) and that LRRK2 is expressed in cerebral cortex and putamen and in extra-cerebral tissues such as lung or heart (Paisan-Ruiz *et al*. 2004; Zimprich *et al*. 2004). However, at the onset of the present study, a complete expression map of these genes in intact tissue was still lacking for both genes. In order to address this issue, we proceeded to elucidate the detailed distribution of PINK1 and LRRK2 mRNA in both mouse and rat brains using non-radioactive *in situ* hybridization histochemistry with riboprobes. Our *in situ* hybridization results for LRRK2 are in line with other very recent studies reported during the course of the submission of the present work (Galter *et al*. 2006; Melrose *et al*. 2006; Simon-Sanchez *et al*. 2006). We further confirmed our findings for both genes by quantitative RT-PCR and for LRRK2 by Western immunoblot. Our results also provide the first neuroanatomical localization of PINK1 mRNA in intact tissue and of LRRK2 protein in tissue homogenates.

Materials and methods

Animals

Ten week old female Wistar rats weighing 190–240 g and eight week old female C57BL/6 J mice weighing 22–24 *g* were housed in a light- and temperature-controlled room (12-h dark : 12-h light cycles) with normal rat or mouse chow and water *ad libitum*. All procedures were conducted in strict accordance with the European Communities Council Directive of 24 November 1986 (86/609/EEC) and were approved by the animal care and use committee of the KULeuven.

Tissue for RNA extracts and protein homogenates

Mice were killed by cervical dislocation and rats were deeply anaesthetized with pentobarbital and then decapitated. Brains were removed from the skull and separate brain regions were rapidly dissected out and snap frozen using liquid nitrogen. Tissues were stored at − 70°C until use for RNA extraction or homogenates.

Total RNA was first extracted from the separate brain regions with the TriZol reagent (Invitrogen, Carlsbad, CA, USA). RNA was further purified using the RNAqueous kit (Ambion, Austin, TX, USA). This purified RNA was subsequently precipitated, washed in 70% ethanol, recovered in distilled water and stored at − 70°C until use in cDNA synthesis.

To make homogenates for use in western immunoblotting, brain regions were homogenized in 5 volumes of buffer medium (10 mM Tris-HCl, 1 mM EDTA, and 0.25 M sucrose pH 7.4), containing a Complete™ protease inhibitor cocktail (Roche Molecular Biochemicals, Indianapolis, IN, USA), using a Potter-Elvehjem homogenizer and a PTFE pestle. An aliquot of the resultant homogenates was stored at − 80°C. The protein content of each preparation was determined by the method of Bradford (Bradford 1976).

Tissue for *in situ* hybridization histochemistry

Mice and rats were deeply anaesthetized with pentobarbital and perfused with 4% paraformaldehyde in PBS. Brains were post-fixed overnight at 4°C and the next day 50 μm thick vibratome sections were collected. Brains were fully sectioned in the frontal plane from rostral to caudal ($N = 4$). During sectioning, brains and sections were kept at 4°C. Sections were placed in a cryopreservation buffer (PBS1x containing 30% ethylene glycol and 30% sucrose) and stored at − 20°C until use in *in situ* hybridization histochemistry.

Quantitative RT-PCR

Primer and probe sequences specific to rat and mouse PINK1 and LRRK2 (table) were selected using Primer Express software (Applied Biosystems, Foster City, CA, USA). Selected sequences were compared to public databases to confirm specificities. Primer pairs were tested using conventional RT-PCR to confirm generation of a single band of the expected amplicon size (not shown). Random primed cDNA was synthesized from 1 μg of total RNA of each brain region in a 40 μL reaction volume using the High Capacity cDNA archive reverse transcription kit (Applied Biosystems). PCR was performed using Applied Biosystems universal master mix containing 200 nM primers and 200 nM probe (FAM label) and the cDNA equivalent of 25 ng of total RNA. Duplicate reactions were run on an Applied Biosystems Prism 7700 sequence detection system and quantified against a standard curve generated from reactions containing serial dilutions of total rat or mouse brain cDNA. The amount of RNA input into each reaction was determined by duplex measurement of GAPDH levels (Applied Biosystems rodent GAPDH quantification kit, VIC labelled probe). Samples were tested for at least two independent cDNA preparations in at least two independent quantitative PCR runs. Data were calculated as relative PINK1 or LRRK2 expression, normalized to GAPDH.

Plasmid constructs

For in situ hybridization probes

Polymerase chain reaction (PCR) primers (see Table 1) were designed based on PINK1 and LRRK2 (GenBank accession numbers: mLRRK2: AY792512, rLRRK2: XM235581, mPINK1: NM026880, rPINK1: XM216565) sequences. PCR for PINK1 probes was performed on commercially available cDNA clones (Open Biosystems, Huntsville, Ala, USA). PCR for LRRK2 probes was performed on a mouse brain cDNA library (for the mouse probe) or on dT primed cDNA from rat striatum (for the rat LRRK2 probe construct, cDNA synthesized in-house).

Table 1 Cloning primers for *in situ* hybridization clones

mPINK1 FW	GCT GTT CGG CTG GGG GAA G
mPINK1 REV	TGG CTT CAT ACA CAG CGG C
rPINK1 FW	GGT GTC AGG CTG GGG CAA
rPINK1 REV	TGG CTT CAT ACA CAG CGG C
mLRRK2 FW	GTC ATG GCA CAG ATC TTG ACA GTG AAG GTG GA
mLRRK2 REV	GTC TAA GAC TTC AGA GCC TAC CAG ACA GTA TGC TT
rLRRK2 FW	CCT GAA GCA TCC TAA GGG CAT
rLRRK2 Rev	CCC ACC AGA CAG TAG GCT TCT

The obtained PCR products were cloned in the pCR4-TOPO (Invitrogen) or pBluescriptII plasmid (Strategene, La Jolla, CA, USA). Sequences were confirmed on both strands using the ABI Prism® BigDye™ Terminator Cycle Sequencing Ready Reaction Kit version 2.0 (Applied Biosystems) with the ABI Prism® 3700 DNA analyzer (Applied Biosystems). The cloned LRRK2 sequences are located in the C-terminal of Ras of complex proteins domain (COR) (452 bp for mouse from position 4663–5115 and 399 bp for rat from position in the coding region of LRRK2). The cloned PINK1 sequences are located mostly outside of the PINK1 kinase domain (439 bp from position 80–519 in the coding region of PINK1, for both rat and mouse probes).

Eukaryotic expression plasmids

Using primers based on human LRRK2 (GenBank accession number AY792511) and oligo dT primed cDNA from SHSY5Y cells, a fragment corresponding to the kinase domain (corresponding to positions 1880–2138 in LRRK2 protein) was amplified and cloned into the pEGFP-C1 plasmid (BD Biosciences Clontech, Mountain View, CA, USA).

In situ hybridization histochemistry

Antisense and sense digoxigenin-labelled riboprobes were produced using T3 and T7 transcription systems and 1 μg of linearized plasmid as previously described (Taymans *et al*. 2004). Riboprobes were recovered in distilled water and stored in aliquots at − 70°C until use.

Sections to be hybridized were quickly rinsed in PBS 1 × at 4°C, then incubated with the following solutions (all at 4°C): PBS1x for 15 min, PBS 1x + 0.1% Triton X-100 for 15 min, HCl 0.02 N for 15 min, Tri-ethanol amine 1.5% and acetic anhydride 25 mM pH 8.0 for 15 min and PBS1x for 3 × 5 min. Sections were then equilibrated in SSC 5x for 15 min and incubated for 1 h in hybridization buffer (SSC 5x, 50% formamide, 5% dextran sulfate, 1 × Denhardt's solution, 250 μg/mL DNA, 100 μg/mL tRNA) in a humid chamber at 65°C for PINK1 sections and 60°C for LRRK2 hybridization. Subsequently, 40 ng heat denatured digoxigenin labelled probe was added to each section.

Following overnight hybridization in a humid chamber (temperatures as above), slides were submitted to the following post-hybridization washes (at the same temperatures as for hybridization): SSC 2x + 50% formamide for 30 min, SSC 2x + 0.3% Triton X-100 for 30 min, SSC 1 × for 30 min and SSC 0.1 × for 3 × 15 min.

Sections were then equilibrated at 22°C in Buffer 1 (100 mM maleic acid, 150 mM NaCl pH 7.5) for 10 min, then incubated for 30 min in Buffer 2 (Buffer 1 containing 1% Roche blocking solution; Roche, Mannheim, Germany). After an overnight incubation at 4°C with alkaline phosphatase-conjugated anti-digoxigenin antiserum (Roche; 1 : 500 in Buffer 2), the sections were quickly rinsed with Buffer 1, then washed for 2 × 10 min in Buffer 1 and equilibrated in Buffer 3 (Tris-HCl 100 mM pH 9.5 with NaCl 100 mM and MgCl2 50 mM) for 10 min. Positive cells were revealed by incubating sections for 4–12 h in the dark at room temperature in an alkaline phosphatase substrate containing solution: Buffer 3 with dimethyl formamide, nitroblue tetrazolium (Roche) and bromo-chloro-indolylphosphate (Roche). The chromogenic reaction was stopped after 1–6 h by rinsing the sections abundantly in Tris-EDTA buffer. Sections were then placed on gelatin-coated microscope slides, dehydrated in an ethanol series, cleared in Histoclear and coverslipped without counterstaining with DPX mountant (Fluka, Bornem, Belgium). As a control of probe specificity, sections hybridized with antisense probe were accompanied by adjacent sections hybridized with sense probe. No significant labelling was observed for any of the sense riboprobes.

Sections processed from *in situ* hybridization histochemistry for PINK1 and LRRK2 were visually examined using a microscope and labelling intensity was scored for each region. Labelling intensity scale: 0, not detected; (+), weak signal; +, moderate signal; + +, strong signal.

Antibody synthesis and western immunoblotting

An anti-LRRK2 antiserum (DR4A/3EDD) was made in rabbits against a keyhole limpet haemocyanin coupled peptide. The peptide sequence corresponds to a sequence in the LRRK2 kinase domain (Cfpnefdeleiqgklpdpv, from pos 2078–96, a cysteine residue was added on the N-terminus for coupling).

Positive controls for antibody validation were generated by transient transfection of plasmids encoding GFP-tagged LRRK2 full length (N- and C-terminal tags, a generous gift of Dr M. Cookson) or kinase domain (LRRK2188c$_{-2138}$, prepared as above) in HEK293T cells. Cells were grown using Dulbecco's Modified Eagle's Medium containing penicillin and streptomycin and supplemented with 10% foetal calf serum. Transfections were performed using poly(ethylenimine), cells were homogenized via sheering through a 30 gauge needle with a 1% SDS solution supplemented with a protease inhibitor cocktail (Roche). Protein content was determined by the method of Bradford (Bradford 1976).

Crude homogenate preparations were diluted in SDS sample buffer containing 10% mercaptoethanol and heated for 5 min at 95°C. For brain homogenates, 20 micrograms of protein per well was resolved on 3–8% Tris-acetate polyacrylamide gels (Invitrogen) in 1 × NuPAGE® Tris-acetate running buffer. For cell culture homogenates, 10 micrograms of protein were resolved on 3–8% Tris-acetate polyacrylamide gels (Invitrogen), as above, or on 12% Tris-glycine polyacrylamide gels in Tris-glycine running buffer. Molecular mass markers (Highmark and Multimark, Invitrogen) were co-electrophoresed for size estimation. Protein was transferred electrophoretically to a polyvinylidenedifluoride (PVDF) membrane in cold transfer buffer containing 10% methanol. The PVDF sheets were blocked in PBS 1 × containing 0.1% Tween 20, 2.5% non-fat dry milk overnight at 4°C and then incubated overnight at 4°C with

anti-LRRK2 serum DR4A/3EDD at a dilution of 1 : 5000 or an anti-GFP serum developed in-house (Baekelandt *et al*. 2003) at a dilution of 1 : 20.000, in PBS plus 2.5% non-fat dry milk. The PVDF sheets were washed in PBS + 0.1% Tween 20 (3 × 10 min) at 22°C followed by incubation for 1 h at 22°C with horseradish peroxidase-conjugated anti-rabbit IgG (1 : 20.000 dilution in PBS + 2.5% non-fat dry milk; Amersham, Arlington Heights, IL, USA). The blots were washed in PBS + 0.1% Tween 20 (2 × 10 min) at 22°C and rinsed in PBS, and immunoreactive proteins were visualized using the enhanced chemiluminescence plus (ECL +) technique (Amersham Pharmacia Biotech, Little Chalfont, England).

Illustrations

Illustrations for the figures of *in situ* hybridization histochemistry were digitally recorded with the Stereo Investigator analyzing system (MicroBrightfield Inc., Williston, VT, USA) connected with a CCD camera to a Leica DMR optical microscope (magnification 1.6–20 ×) as bright-field photomicrographs. Film autoradiograms of western immunoblots were scanned using a Dell 922 flatbed scanner (Dell, Round Rock, TX, USA). Illustrations were prepared with Adobe Photoshop version 5.0.2 (Adobe Systems Incorporated, San Jose, CA, USA) for contrast and brightness adjustments and cropping.

Results

Specificity of the *in situ* hybridization signal

The specificity of the *in situ* hybridization signal was ensured by probe design and verified by processing sections with sense probe. The PINK1 probe was selected in a unique region of its kinase domain. The LRRK2 probe was selected within its COR (C-terminal of Ras of complex proteins) domain, a domain unique to the Roco family of proteins (Bosgraaf and Van Haastert 2003). A BLAST search using our probe sequences yielded significant homologies exclusively for our respective genes of interest. The general specificity of riboprobe hybridization was confirmed by comparing the hybridization signal in sections hybridized with antisense riboprobes to control serial sections hybridized with sense strand probes. These control conditions yielded a low background for the hybridization signals, with no detectable levels in most regions for all controls (inset of Figs 1f–q and 2f–q). Slightly higher background levels were seen with sense control probes for PINK1 in hippocampus and cerebellum. Background levels of sense probe were also higher for LRRK2 in the cerebellum or after extended signal exposure times, such as shown for the substantia nigra (inset Fig. 1j). All brains analyzed showed a similar expression pattern for each probe (4 brains tested for each probe for both mouse and rat).

PINK1 mRNA localization

The PINK1 transcript was expressed throughout the mouse and rat brains, and the distribution pattern was essentially the same in mouse compared to rat brain (the detailed regional distribution is given in Table 3 and illustrated in Fig. 1). Strong hybridization signal was observed in the following regions: layers II–VI of cerebral cortex, striatum, paraventricular hypothalamic nucleus, thalamus, amygdala, hippocampus, mesencephalic nuclei like the substantia nigra, cerebellar cortical areas and pons. Intermediate expression was seen in the globus pallidus while hypothalamic nuclei such as the lateral and ventromedial hypothalamic nuclei displayed generally low expression levels.

The non-radioactive *in situ* hybridization histochemistry method used here allows mRNA localization at the cellular level. For instance, in white matter, PINK1 labeled cells were only very sparsely observed (data not shown). In the cerebellar cortex, cells with high PINK1 levels were seen to be expressed in neurons of the Purkinje cell layer, while granular cell layer cells expressed lower levels of PINK1 mRNA (Fig. 1k,q). In the striatum, the soma size of PINK1 positive cells was found to be approximately 15–20 μm (Fig. 1f,l).

LRRK2 mRNA localization

The LRRK2 transcript was expressed throughout the mouse and rat brains (Table 3, Fig. 2), and the distribution pattern was essentially the same in both rodent species. Strong LRRK2 *in situ* hybridization signal was observed in the following regions: layers II–VI of cerebral cortex, striatum, olfactory tubercle, hippocampus, and amygdala nuclei such as the antero-cortical amygdaloid nucleus and lateral amygdala. Moderate expression was seen in the thalamus, pons and paraventricular hypothalamic nucleus. Septal nuclei showed low (mouse) or moderate (rat) LRRK2 levels, while

Fig. 1 Neuroanatomical distribution of PINK1 mRNA in mouse and rat brain. Frontal mouse and rat brain sections were hybridized with a digoxigenin labelled riboprobe complementary to mouse and rat PINK1, respectively, and further processed as described in the Materials and Methods section. Shown in the first column are representative low magnification bright field photomicrographs of PINK1 *in situ* hybridization histochemistry in the mouse brain at the level of the caudate putamen (a), globus pallidus (b), hippocampus (c), substantia nigra (d) and cerebellum (e). In columns 2 and 3, high magnification images corresponding to boxed areas in overview images are shown for mouse and rat, respectively: caudate putamen (f, l), neocortex (g, m), globus pallidus (h, n), hippocampus (i, o), substantia nigra (j, p) and cerebellar cortex (k, q). The inner diameter of the donut-shape next to the scale bars in panels F and L is 15 μm and corresponds to the average diameter of labelled somata from the caudate-putamen. The block arrows in panels K and Q point to labelled cell somata of Purkinje cells. A full overview of the PINK1 mRNA distributions is presented in Table 3. Scale bars given in the inset sense control images are of the same length as those of the corresponding antisense images. Abbreviations: see list.

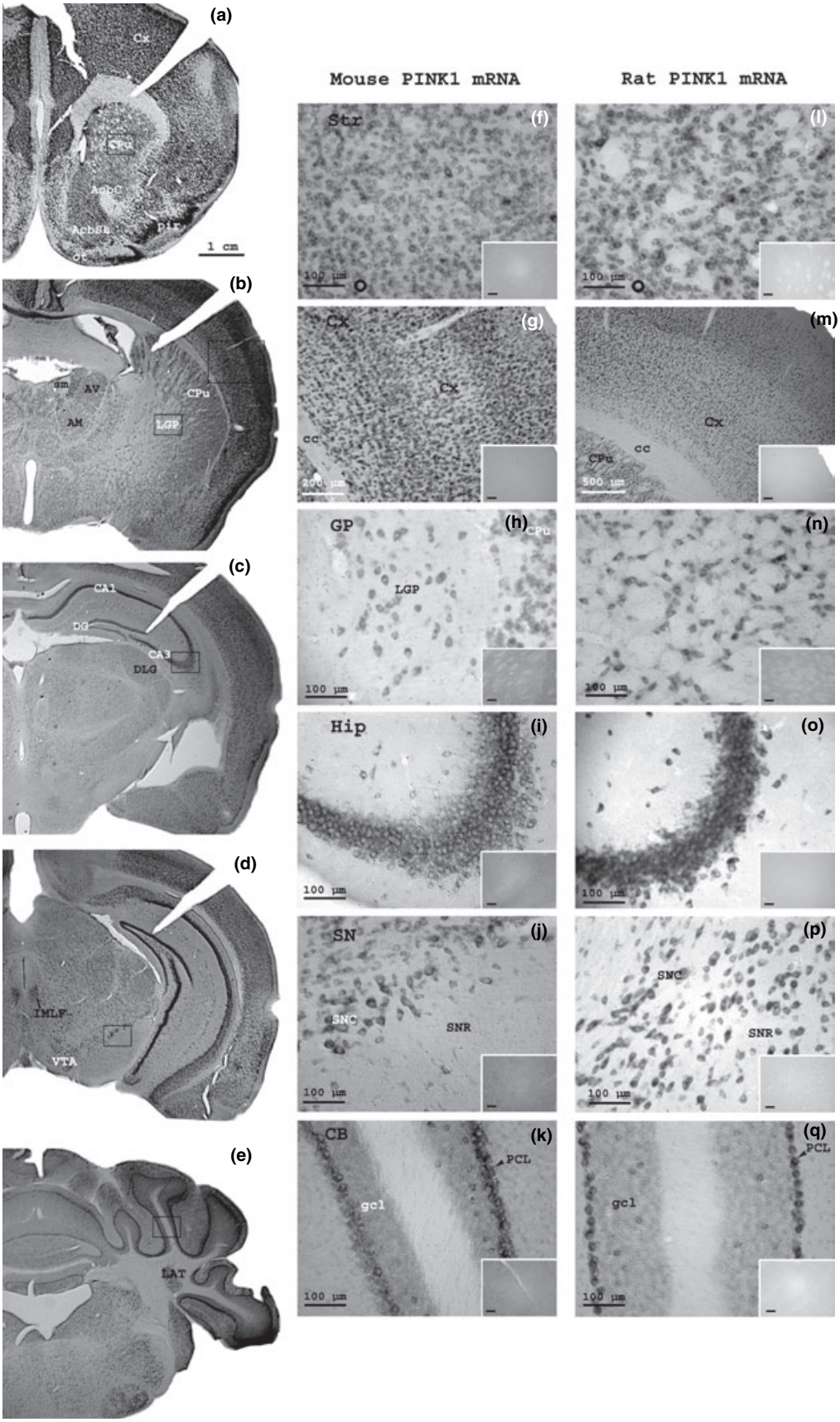

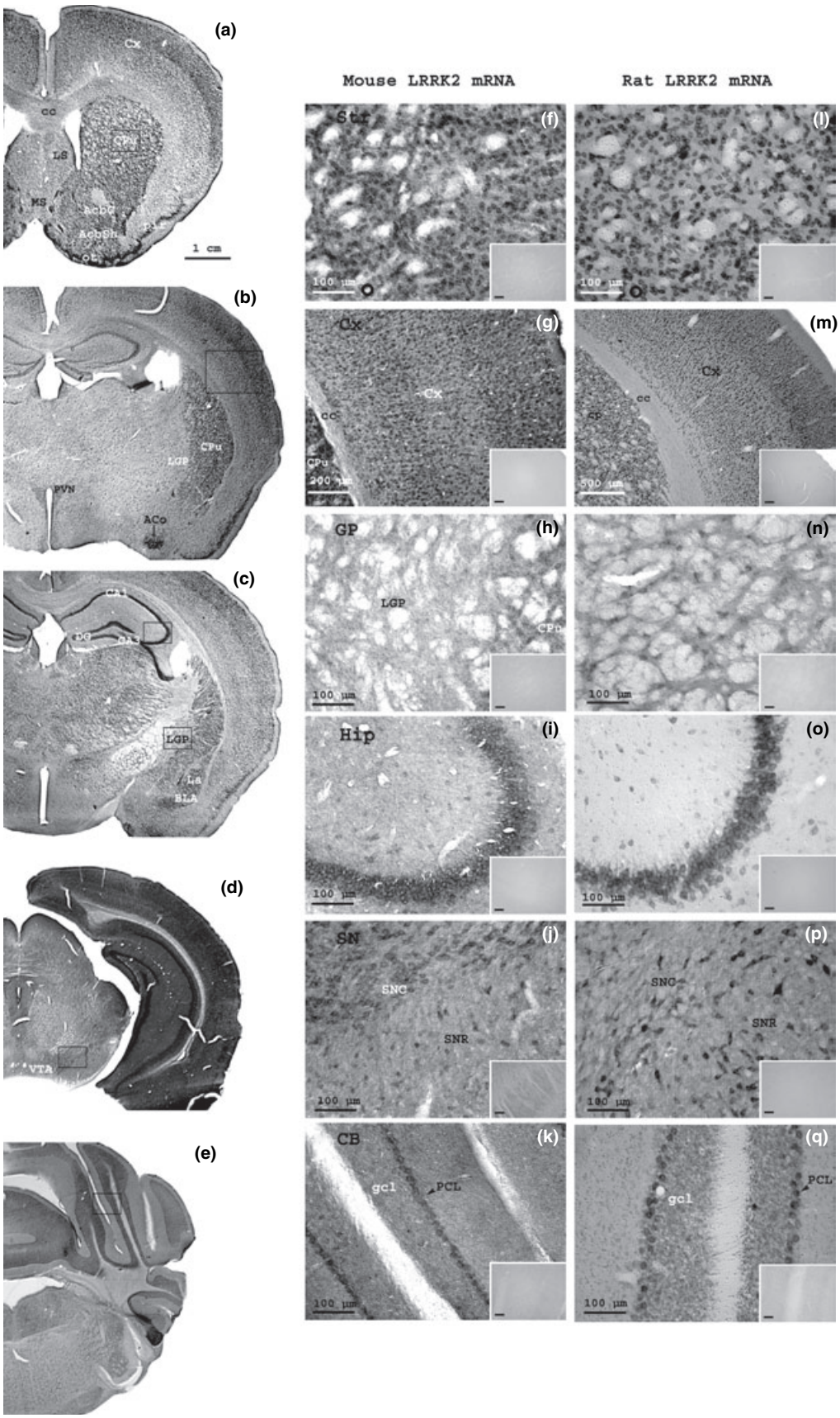

Table 2 Primers and probes used for quantitative RT-PCR

mPINK1 FW	GAG GGC GTG GAC CAT CTG
mPINK1 REV	AGG ATG TTG TCG GAC TTG AGA TC
mPINK probe	Fam-TTC AGC AGG GCA TTG CCC ATC G-Tamra
rPINK1 FW	AGA CGG TCC CAA GCA GCT T
rPINK1 REV	AAG TGA AGG CGC GGA AAA C
rPINK probe	Fam-CCG CAC CCC AAC ATC ATC CG-Tamra
mLRRK2 FW	CAA AGC TTA ATA GGA CCC CAG GAT
mLRRK2 REV	ATT GGC GTG ATG AAC AGT TAA CA
mLRRK2 probe	Fam-TGG GAA GTC CTT GGT ATT CAC CGG CT-Tamra
rLRRK2 FW	CAA AGC TTA ATA GGA CCC CAG GAT
rLRRK2 Rev	GTT GGC ATG ATG AAC AGT TAA CA
rLRRK2 probe	Fam-TGG GAA GTC CTT GGT ATT CAC CGG CT-Tamra

LRRK2 expression in the globus pallidus was either low (rat) or not detected (mouse). Remarkably, LRRK2 expression in the substantia nigra was low as seen in Fig. 2(J,*p*) where revelation of the *in situ* hybridization signal was extended for increased sensitivity (to be compared to 'overexposed' cortical area, Fig. 2d).

At the cellular level, examination of LRRK2-positive cells in the cerebellum revealed that LRRK2 is largely expressed in Purkinje neurons (Fig. 2k,q). In the striatum, the soma size of LRRK2 positive cells was found to be approximately 15–20 μm (Fig. 2f,l).

Quantitative RT-PCR of PINK1 and LRRK2 in regional mouse and rat brain RNA extracts

To obtain more quantitative information on PINK1 and LRRK2 levels, quantitative PCR (see Table 2 for primer/probe sets used) was performed on cDNA of the following rat and mouse brain regions: olfactory bulb, neocortex, striatum, septal region, hypothalamus, diencephalon, mesencephalon, hippocampus, pons and cerebellum. In agreement with the results obtained by *in situ* hybridization histochemistry, quantitative RT-PCR revealed that the PINK1 and LRRK2 genes are widely expressed in mouse and rat brain (Fig. 3). Relative gene expression levels (ratios of gene of interest over the housekeeping gene GAPDH) were equivalent in mouse brain regions compared to rat brain regions for both genes. PINK1 mRNA abundance was similar over all brain regions tested with PINK1/GAPDH ratios ranging between 0.53 and 0.946. LRRK2 mRNA abundance displayed interregional differences with LRRK2/GAPDH ratios ranging from 0.20 (rat hypothalamus) to 5.77 (rat striatum).

Western immunoblot of LRRK2 in regional mouse and rat brain homogenates

In order to examine the protein distribution of LRRK2 in the rodent brain, we developed LRRK2-specific antibodies via immunization of KLH-linked LRRK2 peptides. We assessed the specificity of our primary LRRK2 antiserum (DR4A/3EDD) by several criteria: (1) recognition of GFP-tagged fusion constructs of an LRRK2 fragment (2) recognition of full length LRRK2 and (3) preabsorption tests (Fig. 4a).

The DR4A/3EDD antiserum recognized a band at ~280 kDa in HEK293T cells which express LRRK2 endogenously. In accordance with findings previously reported with another LRRK2 antibody (Giasson *et al*. 2006), our DR4A/3EDD antiserum demonstrated a primary band in the rodent tissue at a slightly lower level (~260 kDa). The strength of the bands varied from region to region, with strong expression seen in the striatum, cortex and hippocampus. Low LRRK2 protein levels were seen in the septum, hypothalamus and olfactory bulb.

Discussion

We have determined the detailed neuroanatomical distribution of PINK1 and LRRK2 in mouse and rat brain using non-radioactive *in situ* hybridization histochemistry. These data are complemented by the quantification of transcript levels in regional brain extracts via quantitative RT-PCR. At the protein level, we examined LRRK2 expression in regional rodent brain homogenates using a specific anti-LRRK2 antiserum raised in house. The main finding of our study is that both genes are expressed throughout the rodent CNS, with PINK1 showing homogeneous expression levels and LRRK2 showing relatively important interregional differences in expression level.

Fig. 2 Neuroanatomical distribution of LRRK2 mRNA in mouse and rat brain. Frontal mouse and rat brain sections were hybridized with a digoxigenin labelled riboprobe complementary to mouse and rat LRRK2, respectively, and further processed as described in the Materials and Methods section. Shown in the first column are representative bright field photomicrographs of LRRK2 *in situ* hybridization histochemistry in the mouse brain at the level of the caudate putamen (a), globus pallidus (b), hippocampus (c), substantia nigra (d) and cerebellum (e). In columns 2 and 3, high magnification images corresponding to boxed areas in overview images are shown for mouse and rat, respectively: caudate putamen (f, l), neocortex (g, m), globus pallidus (h, n), hippocampus (i, o), substantia nigra (j, p) and cerebellar cortex (k, q). The inner diameter of the donut-shape next to the scale bars in panels f and l is 15 μm and corresponds to the average diameter of labelled somata from the caudate-putamen. The block arrows in panels k and q point to labelled cell somata of Purkinje cells. A full overview of the LRRK2 mRNA distributions is presented in Table 3. Scale bars given in the inset sense control images are of the same length as those of the corresponding antisense images. Abbreviations: see list.

Table 3 Distribution of PINK1 and LRRK2 mRNA within the mouse and rat brains

Brain Structure	Mouse PINK1	Rat PINK1	Mouse LRRK2	Rat LRRK2
Telencephalon				
Olfactory bulb	+ +	+ +	(+)	(+)
Neocortex	+ +	+ +	+ +	+ +
Layer I	0	0	0	0
Layer II	+ +	+ +	+ +	+ +
Layer III	+ +	+ +	+ +	+ +
Layer IV	+ +	+ +	+ +	+ +
Layer V	+ +	+ +	+ +	+ +
Layer VI	+ +	+ +	+ +	+ +
Prefrontal cortex	+ +	+ +	+ +	+ +
Piriform cortex	+ +	+ +	+	+ +
Corpus callosum	0	0	0	0
Nucleus accumbens				
Shell	+	+	+ +	+ +
Core	+	+	+ +	+ +
Caudoputamen	+	+	+ +	+ +
Olfactory tubercle	+	+	+ +	+ +
Lateral septum	+	+	(+)	+
Medial septum	+	+	(+)	+
Globus pallidus	+	+	0	(+)
Internal capsule	0	0	0	0
Hippocampus				
CA1 hippocampal field	+ +	+ +	+ +	+ +
CA3 hippocampal field	+ +	+ +	+ +	+ +
Dentate gyrus	+	+	+	+
Amygdala				
Antero-cortical amygdaloid nuc	+	+	+ +	+ +
Amygdalo-striatal transition area	(+)	(+)	+ +	+ +
Lateral amygdala	+ +	+ +	+ +	+ +
Basolateral amygdala	+ +	+	+ +	+ +
Medial amygdala	+	+	+	+
Post-eromedial cortical amygdala	+	+	+	+
Diencephalon				
Medial habenula	+	+	+	+
Lateral habenula	+	(+)	(+)	(+)
Medial lemniscus	0	0	0	0
Thalamus				
Principal relay nuc	+ +	+ +	+	+
Pre-taenial nuc	+	+	+	+
Midline/intralaminar nuc	+	+	+	+
Reticular nuc	+	+ +	+	+
Dorso-lateral geniculate nuc	+ +	+ +	+	+
Ventro-lateral geniculate nuc	+ +	+ +	+	+
Medial geniculate nuc	+	+	+	+
Hypothalamus				
Paraventricular nuc	+ +	+ +	+	+
Ventromedial hypothalamic nuc	0	0	+	(+)
Lateral hypothalamic nuc	(+)	(+)	0	0
Arcuate nuc	(+)	(+)	+	+
Cerebral peduncle	0	0	0	0
Brainstem				
Substantia nigra				
Pars compacta	+	+ +	(+)	(+)
Pars reticulata	+	+	(+)	+
Ventral tegmental area	+	+	+	+
Central gray matter	+	+	+	+
Superior colliculus	+	+	+	+
Inferior colliculus	+	+	+	+
Pontine nuc	+ +	+ +	+	+
Dorsal raphe	+ +	+ +	(+)	(+)
Locus coeruleus	+ +	+ +	(+)	(+)
Cerebellum				
Purkinje cell layer	+ +	+ +	+ +	+ +
Granule cell layer	(+)	(+)	(+)	(+)

Labelling intensity scale: 0, not detected; (+), weak signal; +, moderate signal; + +, strong signal.

For LRRK2, the *in situ* hybridization data presented here is largely consistent with data from other studies published during the course of the submission of the present work (Galter *et al*. 2006; Melrose *et al*. 2006; Simon-Sanchez *et al*. 2006). All three reports show that LRRK2 mRNA is expressed broadly with among others high striatal and cortical expression. Also, our LRRK2 qRT-PCR data is consistent with the study of Melrose and colleagues (Melrose *et al*. 2006). It should be noted that two of these reports using oligoprobes conclude to the absence of LRRK2 mRNA from the substantia nigra, while we detected low nigral levels for LRRK2. This may be explained by our choice to use riboprobes which show higher specificity and sensitivity compared to shorter DNA oligoprobes. Indeed, riboprobes create more stable hybrids than oligoprobes making it possible to employ more stringent hybridization and wash conditions (Tecott *et al*. 1987). Our data are largely in agreement with the study of Simon-Sanchez *et al*. that also uses non-radioactive *in situ* hybridization with riboprobes (Simon-Sanchez *et al*. 2006), except for the rather strong LRRK2 signals we obtained in the nucleus accumbens and the purkinje cells of the cerebellum. The reason for this is unclear, but might be due to differences in mouse strain.

The specificity of our *in situ* hybridization signals given here is further supported by the regional distribution as measured by other methods. The homogeneous expression pattern of PINK1 is confirmed by qRT-PCR. For LRRK2, expression levels seen in the *in situ* hybridization experiments correlate overall to expression levels measured by qRT-PCR or Western blot. For example, all three detection

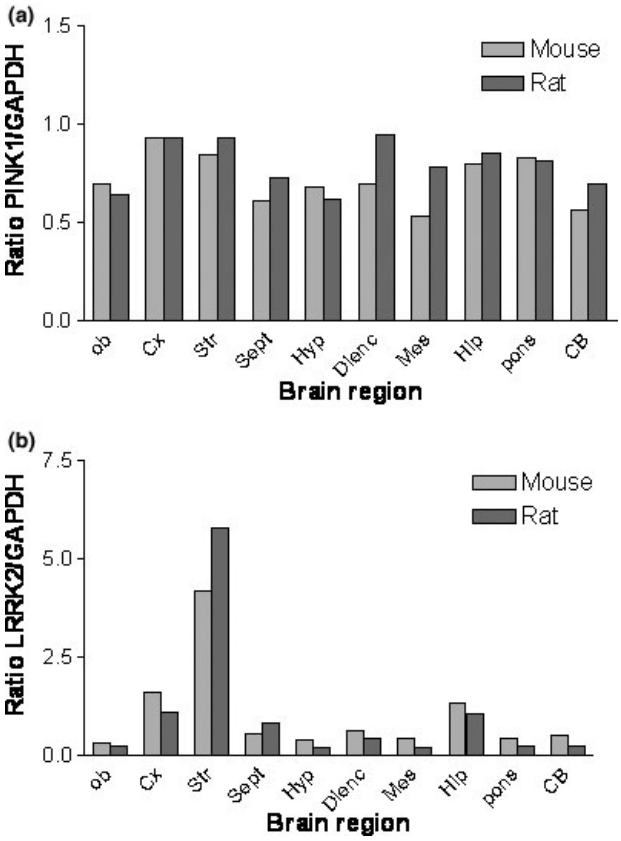

Fig. 3 PINK1 and LRRK2 transcript levels in different rat and mouse brain regions. Quantitative RT-PCR assays for PINK1 (a) and LRRK2 (b) were performed on cDNA from various brain regions. Transcript levels were expressed as a ratio of PINK1 or LRRK2 to the housekeeping gene GAPDH. Note the contrast between the evenly distributed transcript levels for PINK1 and the drastic interregional expression differences for LRRK2. Abbreviations: see list.

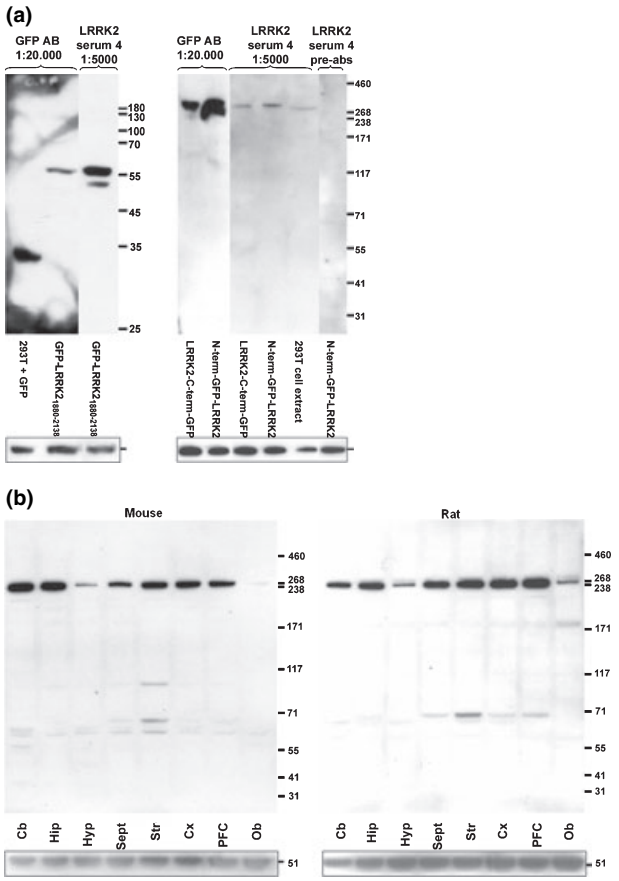

Fig. 4 Western blot analysis of LRRK2 expression in various brain regions and HEK-293T cells. (a) Antibody validation. Extracts of HEK-293T cells transfected with a fusion construct of GFP with LRRK2 kinase domain (LRRK2188c$_{-2138}$) were run on a 12% SDS-polyacrylamide gel. The expressed protein is detected by both a GFP-specific antibody and with our LRRK2-specific serum DR4A/3EDD. Using 3–8% SDS-polyacrylamide gels, serum DR4A/3EDD detected a 280 kDa fragment in extracts from untransfected HEK293T cells. (b) Western blot of mouse and rat brain homogenates. Using 3–8% Tris-acetate SDS-polyacrylamide gels and serum DR4A/3EDD, LRRK2 was detected in various mouse and rat brain tissues as a protein of approximately 260 kDa. As with the *in situ* hybridization and qRT-PCR, striatum, cortex and hippocampus show high LRRK2 expression while hypothalamus, septum and olfactory bulb show lower expression. Immunoblotting for beta-tubulin (51 kDa) is provided as a loading control at the bottom of each blot. Abbreviations: see list.

methods show strong LRRK2 expression in the striatum, cortex and hippocampus and weak LRRK2 expression in the olfactory bulb, septum and hypothalamus. On the other hand, qRT-PCR is the most quantitative method with the widest linear range, which probably explains why the very high LRRK2 signal in the striatum is best seen through this method.

An important issue for further investigation will be to compare the PINK1 and LRRK2 distributions in rodent brain with the distribution in human brain. A study of the distribution of PINK1 mRNA in adult human tissues via Northern blot has shown that PINK1 is expressed in a wide range of tissues including heart, skeletal muscle, testis, kidney and brain (Unoki and Nakamura 2001), however, a regional brain distribution has not yet been described. For LRRK2, gene expression in human tissues as seen via Northern blot and quantitative PCR has also shown that LRRK2 is expressed in a variety of human tissues including heart, lung, kidney and brain (Paisan-Ruiz *et al*. 2004; Zimprich *et al*. 2004). In the brain, the same studies show that LRRK2 is mostly abundant in the putamen and the cerebral cortex with lower levels of expression in the cerebellum and medulla (Paisan-Ruiz *et al*. 2004; Zimprich *et al*. 2004), consistent with our results for mouse and rat brain. In intact human brain tissue, LRRK2 protein expression was demonstrated in Purkinje cells of the cerebellum (Giasson *et al*. 2006), as we show here for LRRK2 mRNA in mouse and rat. Galter and colleagues have recently shown

that LRRK2 mRNA levels in human cortex and striatum are high while nigral levels are very low or absent (Galter *et al*. 2006), findings which are in line with our results in mouse and rat. It would be interesting to extend these data to other regions of the human brain such as amygdala nuclei or the hippocampus which show high LRRK2 expression in rodents.

Although the precise cell types expressing PINK1 and LRRK2 remain to be conclusively determined, our data are consistent with neuronal expression of PINK1 and LRRK2. Both genes are expressed exclusively in grey matter regions with no or very sparse labeling in white matter and both PINK1 and LRRK2 expression is seen in neuronal Purkinje cells (Figs 1k,q and 2k,q). In the striatum, both genes are expressed in cells with a soma diameter of 15–20 μm, consistent with the soma size of striatal medium spiny neurons (Gerfen 2004), but excluding expression in cells with small soma size such as microglia. Medium spiny neurons comprise 95% of the striatal neurons, with approximately half accounting for direct pathway (striatonigral) projections and the other half to the indirect (striatopallidal) pathway (Gerfen 2004). Further studies including colocalization of PINK1 or LRRK2 with neuronal and glial markers will be necessary to formally determine the cell types expressing these two genes.

A striking finding of this study is that both PINK1 and LRRK2 show a broad distribution of gene expression while pathogenicity in Parkinson's disease is much localized. Indeed, the hallmark of Parkinson's disease is neuronal degeneration in the dopaminergic neurons of the substantia nigra (Kish *et al*. 1988), a feature which may be accompanied by additional histopathological features such as brainstem or cortical Lewy bodies. Nigral neuron degeneration has been shown indirectly via positron emission tomography in carriers of PINK1 disease mutations (Khan *et al*. 2002) and in carriers of LRRK2 clinical mutations (Adams *et al*. 2005; Hernandez *et al*. 2005). For LRRK2 PD patients, this has been confirmed in postmortem histopathological studies (Zimprich *et al*. 2004; Giasson *et al*. 2006; Ross *et al*. 2006). Interestingly, the distribution of other genes linked to familial Parkinson's disease such as alpha-synuclein (Hong *et al*. 1998), parkin (D'Agata *et al*. 2000; Stichel *et al*. 2000) or DJ-1 (Shang *et al*. 2004; Bader *et al*. 2005) also show a broad distribution. The apparent contradiction between a broad expression pattern and the involvement in anatomically localized degeneration may be reconciled by the notion that PINK1 and LRRK2 cellular function could be regulated differently from one functional cell group to another. For LRRK2, its low level of expression in the substantia nigra raises the possibility that its potential role in nigral degeneration may be carried out at the systems level rather than at the cellular level. Expression of LRRK2 is highest in the striatum, a region which is in direct contact with the substantia nigra via mutual projections. Region-specific action of PINK1 or LRRK2 may also be regulated by region–specific interactions with other genes. So far, no physical interaction partners have been described for PINK1. Interestingly, LRRK2 has been shown to interact with parkin *in vitro* and following transient transfection in HEK293T cells (Smith *et al*. 2005). Expression of LRRK2 and parkin overlaps in several regions of the rodent brain such as cortex, hippocampus or cerebellar Purkinje cells (D'Agata *et al*. 2000; Stichel *et al*. 2000). However, on the contrary to LRRK2, parkin is not expressed in the rodent caudate-putamen, indicating that the parkin–LRRK2 interaction may not be essential to LRRK2 function.

In summary, we show here that both PINK1 and LRRK2 are broadly expressed in the rodent brain with expression of both genes in structures relevant to PD: substantia nigra, caudate-putamen, cortex, hippocampus. Distribution patterns were the same in both rat and mouse and were consistent with neuronal expression. Our study provides an important basis for the future study of the roles of PINK1 and LRRK2 in the brain.

Acknowledgements

Eukaryotic expression constructs of GFP-tagged human LRRK2 were a generous gift of Dr M. Cookson. The authors thank Anke Van der Perren for assistance in LRRK2 antibody development and Elke Van Rompay for assistance in antibody validation. The authors also thank Dr Rik Gijsbers for technical advice, Kristel Eggermont for assistance in optimizing the *in situ* hybridization protocol and Lies Dekeyzer and Frea Coun for technical assistance. V.B. is a postdoctoral fellow of the Flemish Fund for Scientific Research (FWO Vlaanderen). This work was supported by the FWO Vlaanderen (G.0164.03, G.0406.06), the Institute for the Promotion of Innovation by Science and Technology in Flanders (IWT SBO/030238) the European Community (NEUROPARK, QLK3-CT-2002–02114, DiMI LSHB-CT- 2005–512146) and the Michael J Fox Foundation for Parkinson's Research.

References

Adams J. R., van Netten H., Schulzer M., Mak E., McKenzie J., Strongosky A., Sossi V., Ruth T. J., Lee C. S., Farrer M., Gasser T., Uitti R. J., Calne D. B., Wszolek Z. K. and Stoessl A. J. (2005) PET in LRRK2 mutations: comparison to sporadic Parkinson's disease and evidence for presymptomatic compensation. *Brain* **128**, 2777–2785.

Bader V., Ran Z. X., Lubbert H. and Stichel C. C. (2005) Expression of DJ-1 in the adult mouse CNS. *Brain Res.* **1041**, 102–111.

Baekelandt V., Eggermont K., Michiels M., Nuttin B. and Debyser Z. (2003) Optimized lentiviral vector production and purification procedure prevents immune response after transduction of mouse brain. *Gene Ther.* **23**, 1933–1940.

Bosgraaf L. and Van Haastert P. J. (2003) Roc, a Ras/GTPase domain in complex proteins. *Biochim. Biophys. Acta* **1643**, 5–10.

Bradford M. M. (1976) A rapid and sensitive method for the quantitation of microgram quantities of protein utilizing the principle of protein-dye binding. *Anal Biochem.* **72**, 248–254.

D'Agata V., Zhao W. and Cavallaro S. (2000) Cloning and distribution of the rat parkin mRNA. *Brain Res. Mol Brain Res.* **75**, 345–349.

Galter D., Westerlund M., Carmine A., Lindqvist E., Sydow O. and Olson L. (2006) LRRK2 expression linked to dopamine-innervated areas. *Ann. Neurol.* **59**, 714–719.

Gasser T. (2005) Genetics of Parkinson's disease. *Curr. Opin. Neurol.* **18**, 363–369.

Gerfen C. R. (2004) Basal Ganglia. In: *The Rat Nervous System* (Paxinos, G., ed.), pp. 455–507. Elsevier, San Diego, USA.

Giasson B. I., Covy J. P., Bonini N. M., Hurtig H. I., Farrer M. J., Trojanowski J. Q. and Van Deerlin V. M. (2006) Biochemical and pathological characterization of Lrrk2. *Ann. Neurol.* **59**, 315–322.

Gloeckner C. J., Kinkl N., Schumacher A., Braun R. J., O'neill E., Meitinger T., Kolch W., Prokisch H. and Ueffing M. (2005) The Parkinson disease causing LRRK2 mutation I2020T is associated with increased kinase activity. *Hum Mol Genet* **15**, 223–232.

Hatano Y., Li Y., Sato K., Asakawa S., Yamamura Y., Tomiyama H., Yoshino H., Asahina M., Kobayashi S., Hassin-Baer S., Lu C. S., Ng A. R., Rosales R. L., Shimizu N., Toda T., Mizuno Y. and Hattori N. (2004) Novel PINK1 mutations in early-onset parkinsonism. *Ann. Neurol.* **56**, 424–427.

Healy D. G., Abou-Sleiman P. M., Gibson J. M., Ross O. A., Jain S., Gandhi S., Gosal D., Muqit M. M., Wood N. W. and Lynch T. (2004) PINK1 (PARK6) associated Parkinson disease in Ireland. *Neurology* **63**, 1486–1488.

Hernandez D. G., Paisan-Ruiz C., McInerney-Leo A., Jain S., Meyer-Lindenberg A., Evans E. W., Berman K. F., Johnson J., Auburger G., Schaffer A. A., Lopez G. J., Nussbaum R. L. and Singleton A. B. (2005) Clinical and positron emission tomography of Parkinson's disease caused by LRRK2. *Ann. Neurol.* **57**, 453–456.

Hong L., Ko H. W., Gwag B. J., Joe E., Lee S., Kim Y. T. and Suh Y. H. (1998) The cDNA cloning and ontogeny of mouse alpha-synuclein. *Neuroreport* **9**, 1239–1243.

Khan N. L., Valente E. M., Bentivoglio A. R., Wood N. W., Albanese A., Brooks D. J. and Piccini P. (2002) Clinical and subclinical dopaminergic dysfunction in PARK6-linked parkinsonism: an 18F-dopa PET study. *Ann. Neurol.* **52**, 849–853.

Kish S. J., Shannak K. and HornykiewicZ. O. (1988) Uneven pattern of dopamine loss in the striatum of patients with idiopathic Parkinson's disease. Pathophysiologic and clinical implications. *N Engl. J. Med.* **318**, 876–880.

Mata I. F., Kachergus J. M., Taylor J. P., Lincoln S., Aasly J., Lynch T., Hulihan M. M., Cobb S. A., Wu R. M., Lu C. S., LahoZ. C., Wszolek Z. K. and Farrer M. J. (2005) Lrrk2 pathogenic substitutions in Parkinson's disease. *Neurogenetics* **6**, 171–177.

Melrose H., Lincoln S., Tyndall G., Dickson D. and Farrer M. (2006) Anatomical localization of leucine-rich repeat kinase 2 in mouse brain. *Neuroscience* **139**, 791–794.

Nakajima A., Kataoka K., Hong M., Sakaguchi M. and Huh N. H. (2003) BRPK, a novel protein kinase showing increased expression in mouse cancer cell lines with higher metastatic potential. *Cancer Lett.* **201**, 195–201.

Paisan-Ruiz C., Jain S., Evans E. W., Gilks W. P., van der Simon J. B. M., de Munain A. L., Aparicio S., Gil A. M., Khan N., Johnson J., Martinez J. R., Nicholl D., Carrera I. M., Pena A. S., de Silva R., Lees A., Marti-Masso J. F., Perez-Tur J., Wood N. W. and Singleton A. B. (2004) Cloning of the gene containing mutations that cause PARK8-linked Parkinson's disease. *Neuron* **44**, 595–600.

Rogaeva E., Johnson J., Lang A. E., Gulick C., Gwinn-Hardy K., Kawarai T., Sato C., Morgan A., Werner J., Nussbaum R., Petit A., Okun M. S., McInerney A., Mandel R., Groen J. L., Fernandez H. H., Postuma R., Foote K. D., Salehi-Rad S., Liang Y., Reimsnider S., Tandon A., Hardy J., George-Hyslop P. and Singleton A. B. (2004) Analysis of the PINK1 gene in a large cohort of cases with Parkinson disease. *Arch. Neurol.* **61**, 1898–1904.

Rohe C. F., Montagna P., Breedveld G., Cortelli P., Oostra B. A. and Bonifati V. (2004) Homozygous PINK1 C-terminus mutation causing early-onset parkinsonism. *Ann. Neurol.* **56**, 427–431.

Ross O. A., Toft M., Whittle A. J., Johnson J. L., Papapetropoulos S., Mash D. C., Litvan I., Gordon M. F., Wszolek Z. K., Farrer M. J. and Dickson D. W. (2006) Lrrk2 and Lewy body disease. *Ann. Neurol.* **59**, 388–393.

Shang H., Lang D., Jean-Marc B. and Kaelin-Lang A. (2004) Localization of DJ-1 mRNA in the mouse brain. *Neurosci. Lett.* **367**, 273–277.

Simon-SancheZ. J., Herranz-Perez V., Olucha-Bordonau F. and Perez-Tur J. (2006) LRRK2 is expressed in areas affected by Parkinson's disease in the adult mouse brain. *Eur J. Neurosci.* **23**, 659–666.

Smith W. W., Pei Z., Jiang H., Moore D. J., Liang Y., West A. B., Dawson V. L., Dawson T. M. and Ross C. A. (2005) Leucine-rich repeat kinase 2 (LRRK2) interacts with parkin, and mutant LRRK2 induces neuronal degeneration. *Proc. Natl Acad. Sci. USA* **102**, 18 676–18 681.

Stichel C. C., Augustin M., Kuhn K., Zhu X. R., Engels P., Ullmer C. and Lubbert H. (2000) Parkin expression in the adult mouse brain. *Eur J. Neurosci.* **12**, 4181–4194.

Taymans J.-M., Kia H. K., Claes R., Cruz C., Leysen J. E. and Langlois X. (2004) Dopamine receptor mediated regulation of RGS2 and RGS4 mRNA differentially depends on ascending dopamine projections and time. *European J. Neuroscience* **19**, 2249–2260.

Tecott L. H., Eberwine J. H., Barchas J. D. and Valentino K. L. (1987) Methodological Considerations in the Utilization of In Situ Hybridization. In: *Situ Hybridization: Applications to Neurobiology* (Valentino, K. L., Eberwine, J. H. and Barchas, J. D., eds), pp. 3–24. Oxford University Press, New York.

Unoki M. and Nakamura Y. (2001) Growth-suppressive effects of BPOZ. and EGR2, two genes involved in the PTEN signaling pathway. *Oncogene* **20**, 4457–4465.

Valente E. M., Abou-Sleiman P. M., Caputo V., Muqit M. M., Harvey K., Gispert S., Ali Z., Del Turco D., Bentivoglio A. R., Healy D. G., Albanese A., Nussbaum R., Gonzalez-Maldonado R., Deller T., Salvi S., Cortelli P., Gilks W. P., Latchman D. S., Harvey R. J., Dallapiccola B., Auburger G. and Wood N. W. (2004) Hereditary early-onset Parkinson's disease caused by mutations in PINK1. *Science* **304**, 1158–1160.

West A. B., Moore D. J., Biskup S., Bugayenko A., Smith W. W., Ross C. A., Dawson V. L. and Dawson T. M. (2005) Parkinson's disease-associated mutations in leucine-rich repeat kinase 2 augment kinase activity. *Proc. Natl Acad. Sci. U S A* **102**, 16 842–16 847.

Zimprich A., Biskup S., Leitner P., Lichtner P., Farrer M., Lincoln S., Kachergus J., Hulihan M., Uitti R. J., Calne D. B., Stoessl A. J., Pfeiffer R. F., Patenge N., Carbajal I. C., Vieregge P., Asmus F., Muller-Myhsok B., Dickson D. W., Meitinger T., Strom T. M., Wszolek Z. K. and Gasser T. (2004) Mutations in LRRK2 cause autosomal-dominant parkinsonism with pleomorphic pathology. *Neuron* **44**, 601–607.

